Cell Metabolism, Volume *28*

Supplemental Information

Short-Term Fasting Reveals Amino Acid Metabolism as a Major Sex-Discriminating Factor in the Liver

Sara Della Torre, Nico Mitro, Clara Meda, Federica Lolli, Silvia Pedretti, Matteo Barcella, Luisa Ottobrini, Daniel Metzger, Donatella Caruso, and Adriana Maggi

Figure S1, related to Figure 1

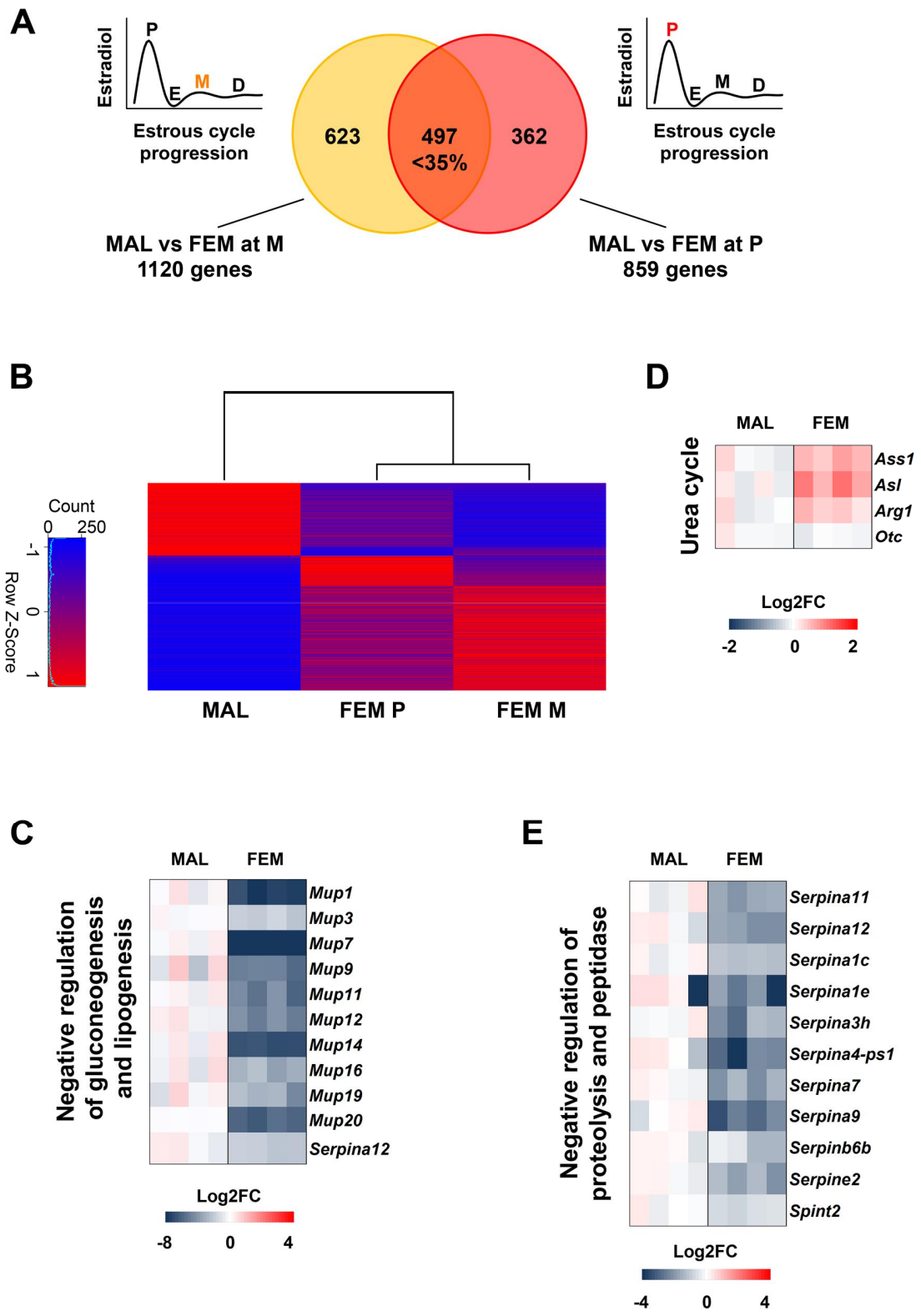

Figure S1: Liver transcriptome in female mice changes in relation to the phase of the estrous cycle (related to Figure 1)

A. Venn diagram summarizing the overlap between DEGs (with |FC|>1.5 and FDR<0.01) measured by RNA-Seq in the liver of males and females at Metestrus (M, yellow circle on the left) and in the liver of males and females at Proestrus (P, red circle on the right).

B. Heatmap showing the clustering of the DEGs from RNA-Seq analysis performed in the livers of males and females at M and P. The heatmap has been generated from the mean value of each DEG using the web interface shinyheatmap (http://shinyheatmap.com/).

(C-E). Heatmap reporting as Log_2 fold change the expression of genes associated with negative regulation of gluconeogenesis and lipid metabolism (**C**), urea cycle (**D**), and negative regulation of proteolysis and peptidase activity (**E**) from RNA-Seq analysis performed in the livers of males and females at M.

Figure S2, Related to Figure 2

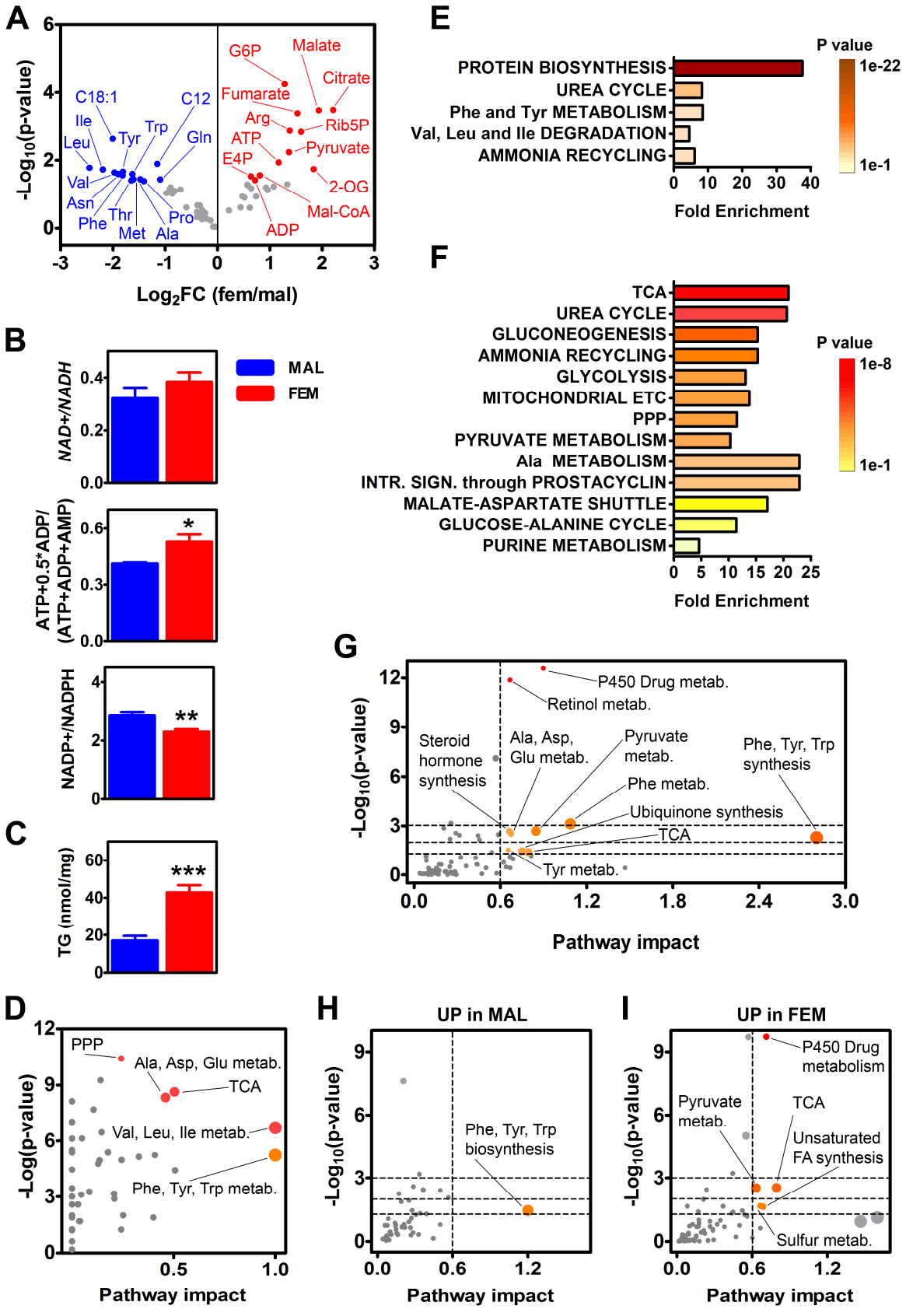

Figure S2: Unsupervised bioinformatics analysis of male and female liver after short-term fasting (Related to Figure 2)

A. Volcano plot of biologically relevant metabolites measured in the liver of males and females at M. Metabolites with significantly upregulated expression in males and females are colored in blue and red, respectively; other metabolites are displayed in gray.

B. Relative changes in NAD^+/NADH ratio (upper), $NADP^+$/NADPH ratio (middle) and energy charge expressed as (ATP+0.5*ADP)/(ATP+ADP+AMP) (lower) in the livers of males and females at M.

The data are Mean ± SEM (n=6). *p<0.05 and **p<0.01 *vs* MAL.

C. Triglyceride (TG) content measured in the livers of males and females at M. The data are Mean ± SEM (n=10-12). ***p<0.001 *vs* MAL.

D. Pathway impact analysis of the biological pathways regulated in the livers of males and females at M. The metabolic pathways are represented as circles according to their enrichment (p-value, Y axis) and topology analyses (pathway impact, X axis) using MetaboAnalyst 3.0 software. The color of each metabolic pathway is related to the p-value obtained from enrichment analysis and its size represents the fold enrichment score; darker circle colors indicate more significant changes of metabolites in the corresponding pathway. The size of the circle corresponds to the pathway impact score and is correlated with the centrality of the involved metabolites.

(E-F). Fold enrichment analysis by MetaboAnalyst 3.0 software of the pathways up-regulated in the livers of males (**E**) and females at M (**F**).

G. Differentially regulated pathways in the livers of males and females at M performed by integrating metabolomic and transcriptomic data with the MetaboAnalyst 3.0 software. The biological pathways are represented as circles according to their enrichment (p-value, Y axis) and topology analyses (pathway impact, X axis). For the integrative analysis only pathways with a ï Log10(p-value) greater than 1.3 and a topology index (pathway impact) greater than 0.6 were taken into account as significant.

(H-I). Integrative analysis performed on the up-regulated genes and metabolites measured in the livers of males (**H**) and females at M (**I**).

Figure S3, Related to Figure 4

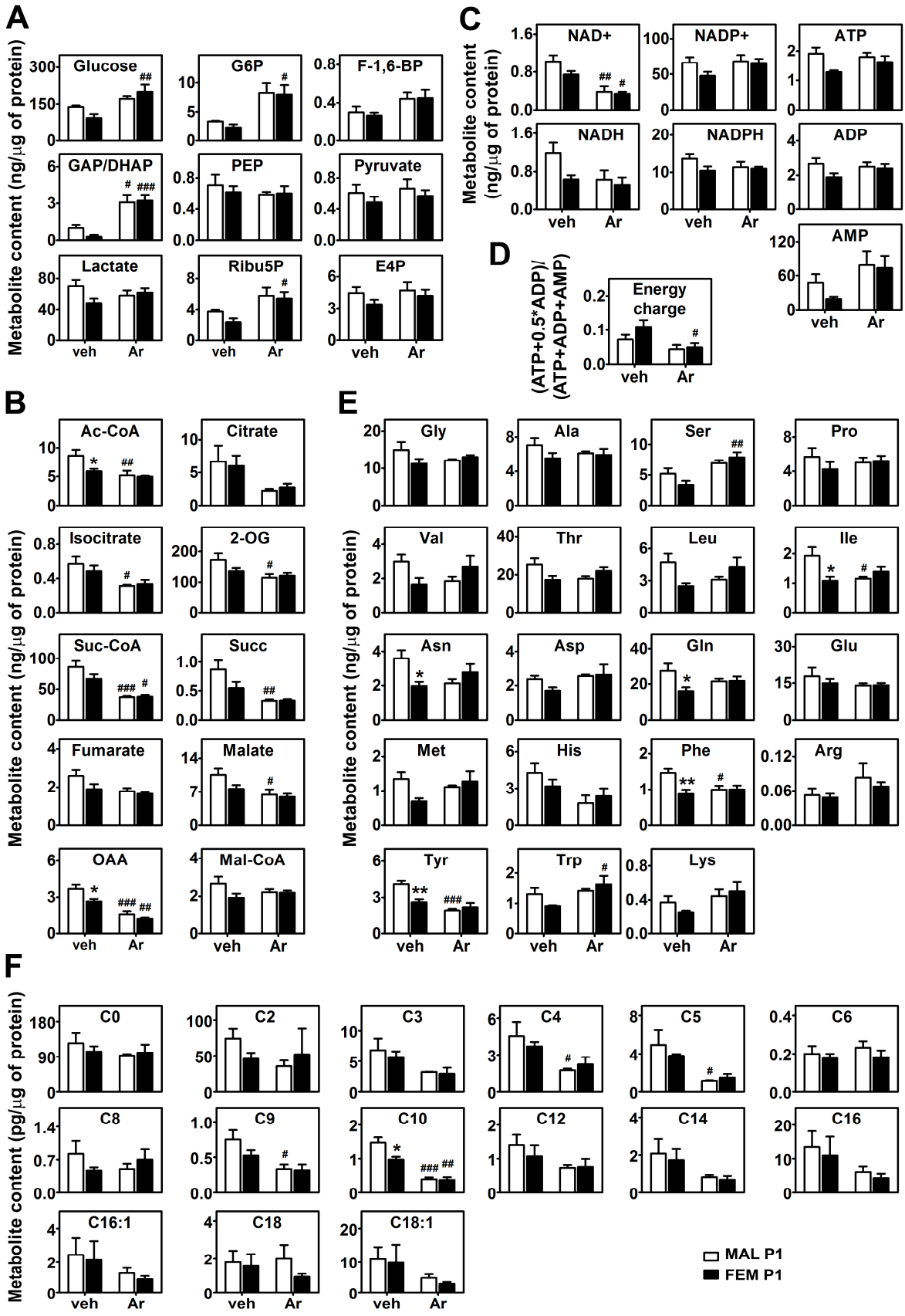

Figure S3: Quantitative analysis of metabolites present in the liver of male and female mice at P1 (Related to Figure 4)

(A-C). Content of biologically relevant metabolites belonging to glycolysis/gluconeogenesis and PPP (**A**), TCA and lipogenesis (**B**), and energy metabolism (**C**) measured in the liver of male and female mice at P1 after treatment with vehicle (veh) or Arimidex (Ar, 1 mg/kg/day).

D. Energy charge values measured in the liver of male and female mice at P1 after treatment with vehicle (veh) or Arimidex (Ar, 1mg/kg/day).

(E,F). Content of amino acids (**E**) and acyl-carnitines (**F**) measured in the liver of male and female mice at P1 after treatment with vehicle (veh) or Arimidex (Ar, 1mg/kg/day).

Data represent the Mean ± SEM (n= 3-5). *p<0.05 and **p<0.01 *vs* MAL; #p<0.05, ##p<0.01 and ###p<0.001 *vs* veh.

Figure S4, Related to Figure 5

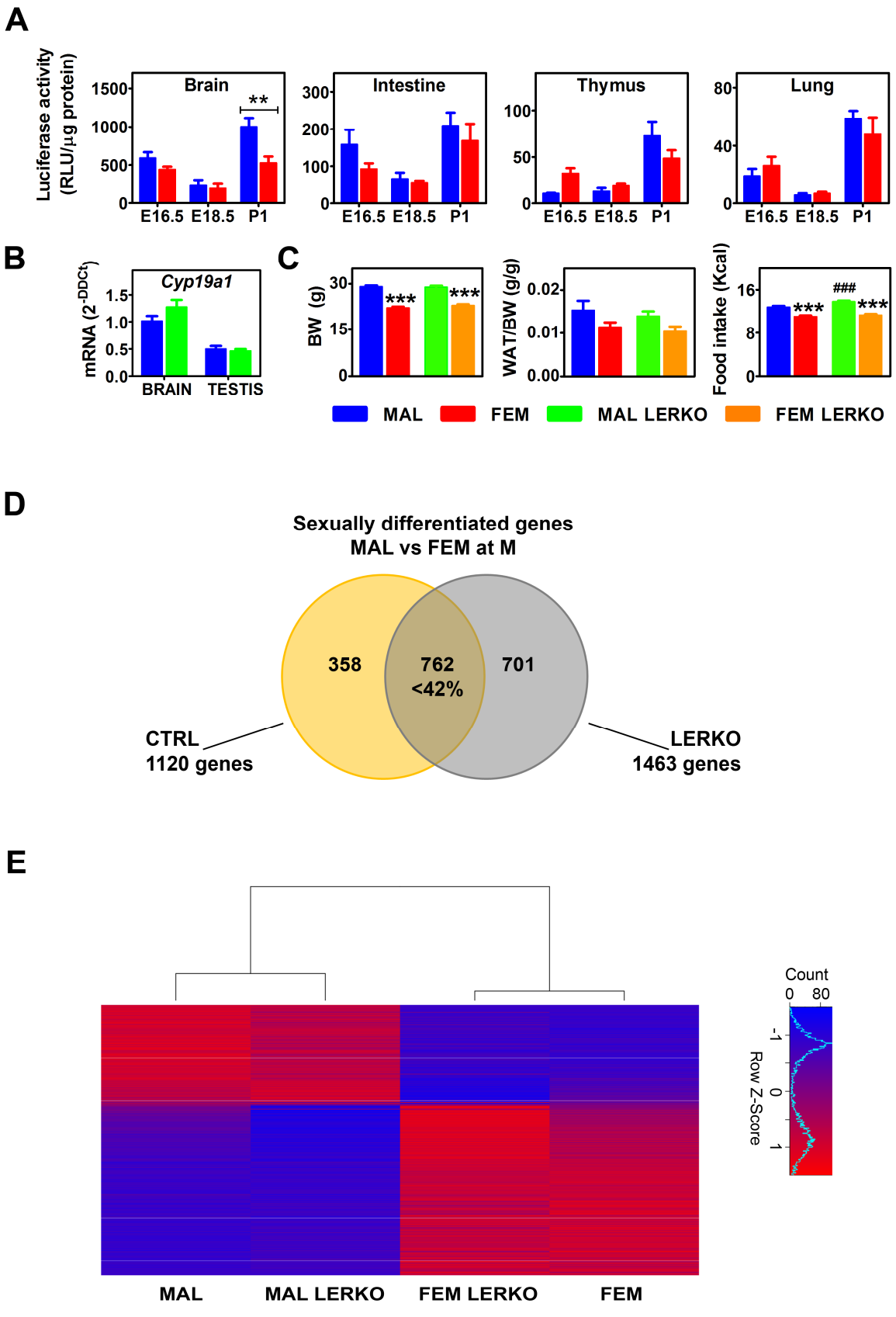

Figure S4: Developmental changes in Estrogen Receptor transcriptional activation in ERE-Luc mice and metabolic phenotype of liver-specific ERα ablation (Related to Figure 5 and 6).

A. Luciferase enzymatic activity measured in the brain, intestine, thymus and lung of male and female ERE-Luc mice at embryonal day 16.5 (E16.5) and 18.5 (E18.5) and postnatal day 1 (P1). Data represent Mean ± SEM (n=2-11). ***p<0.001 by two-way Anova followed by Bonferroni *post hoc* test.

B. The *Cyp19a1* mRNA content was measured by real-time PCR in the brain and testis of males (MAL) and LERKO males (LERKO MAL) at P1. Data represent Mean ± SEM (n=5).

C. Body weight (BW), white adipose tissue (WAT) weight normalized on BW and food intake of males (MAL), females (FEM), LERKO males (LERKO MAL) and LERKO females (LERKO FEM). Data represent Mean ± SEM (n=17-29). ***p<0.001 *vs* MAL and ###p<0.001 *vs* control mice by two-way Anova followed by Bonferroni *post hoc* test.

D. Venn diagram summarizing the overlap between DEGs (with |FC|>1.5 and FDR<0.01) measured by RNA-Seq in the liver of control males and females at M (yellow circle on the left) and LERKO males and females at M (gray circle on the right).

E. Heatmap showing the clustering of the DEGs from RNA-Seq analysis performed in the livers of males and females control and LERKO mice by using the web interface shinyheatmap (http://shinyheatmap.com/).

Figure S5, Related to Figure 6

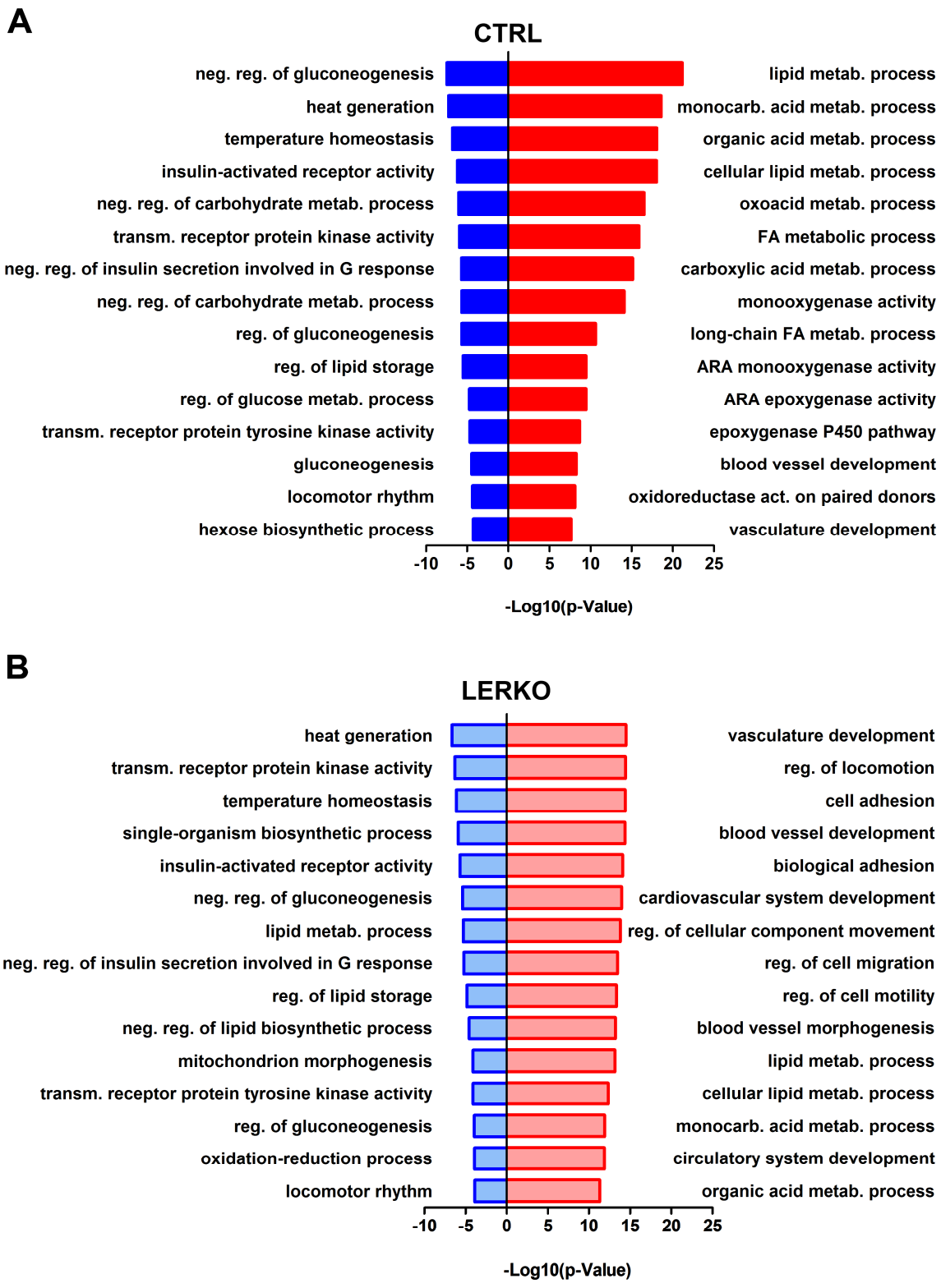

Figure S5: Functional profiling of sexually dimorphic genes in the liver of control and LERKO mice (Related to Figure 6).

Functional profiling of sexually dimorphic genes from RNA-Seq analysis in the liver of CTRL and LERKO mice by g:Profiler (http://biit.cs.ut.ee/gprofiler/). We took into consideration the top 15 most significantly enriched Gene ontology (GO) terms in biological process and molecular function.

A. GO analysis related to the genes up-regulated in the liver of control males (blue bars) and of control females at M (red bars).

B. GO analysis of the genes-regulated in the liver of LERKO males (blue light bars) and of LERKO females at M (red light bars).

Figure S6, Related to Figure 6

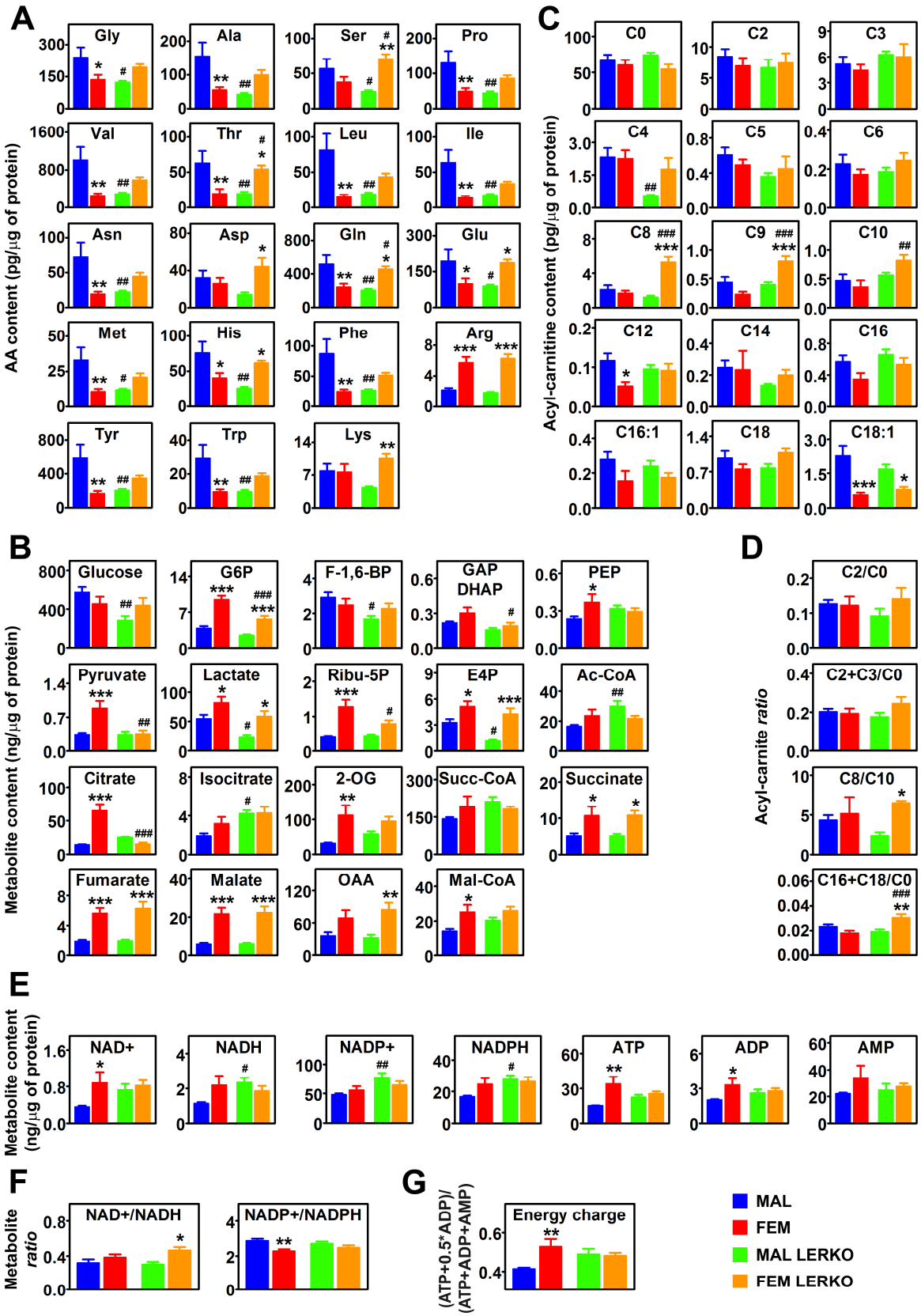

Figure S6: Sex-specific impact of hepatic ERα ablation on liver metabolome (Related to Figure 6).

A. AA content measured in the liver of male and female control (ERα floxed) and LERKO mice.

B. Content of metabolite of the glycolysis/gluconeogenesis, PPP, TCA, and lipogenesis measured in the liver of male and female control and LERKO mice.

C. Quantitative analysis of acyl-carnitines.

D. Relative abundance of acyl-carnitines. The C2/C0 and C2+C3/C0 *ratio* are a measure of overall ß-oxidation activity; the C8/C10 *ratio* is an indicator of an impairment in the oxidation of medium-chain FA; the C16+C18/C0 *ratio* reports the activity of carnitine palmitoyltransferase l (Cpt1α), the rate-limiting step in the uptake of FA into mitochondria.

E. Quantitative analysis of energy related metabolites in the liver of male and female control and LERKO mice.

F. *Ratio* of nicotinamide metabolites (NAD+/NADH and NADP+/NADPH) and energy charge values (expressed as ATP+0.5*ADP/(ATP+ADP+AMP)) .

Data represent the Mean ± SEM (n=6). *p<0.05, **p<0.01 and ***p<0.001 *vs* MAL; #p<0.05, ##p<0.01 and ###p<0.001 *vs* control mice.

Figure S7, Related to Figure 6

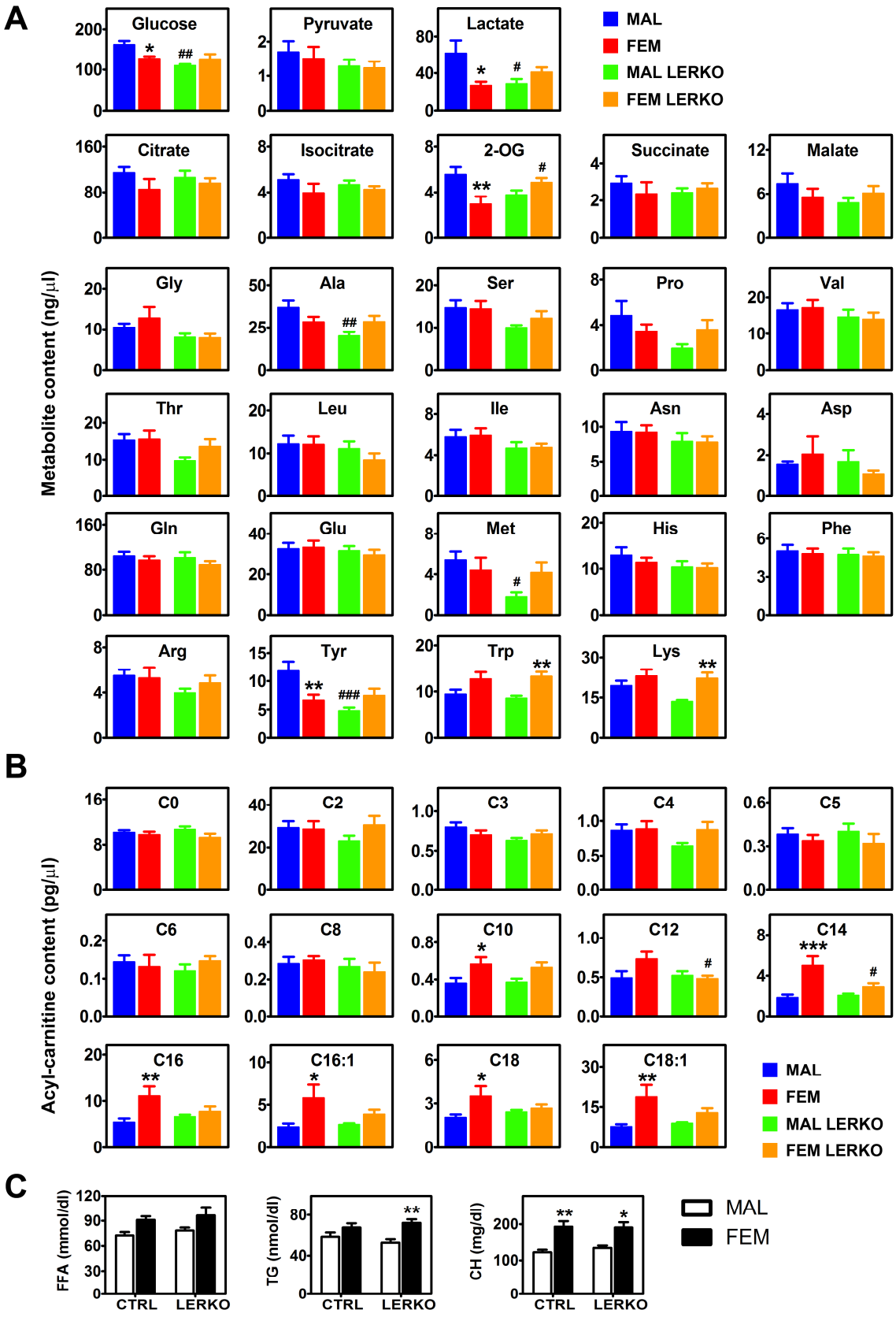

Figure S7: Quantitative analysis of the metabolites present in the plasma of control and LERKO mice (Related to Figure 6).

A. Quantitative analysis of the metabolites of the glycolysis/gluconeogenesis, TCA, and AA.

B. Plasma Acetyl-carnitine content.

Data represent the Mean ± SEM (n=6). *p<0.05, **p<0.01 and ***p<0.001 *vs* MAL; #p<0.05, ##p<0.01 and ###p<0.001 *vs* control mice.

C. Free fatty acids (FFA), triglyceride (TG) and cholesterol (CH) content measured in the plasma of control and LERKO males and females at M. The data are Mean ± SEM, n=10-14. *p<0.05 and **p<0.01 *vs* MAL.

Table S1. Abbreviations of metabolites used in Figures 2, 4, 5, 7 and S2, S3, S6, and S7.

Short name	Full metabolite name	Pathway/Class
Glucose	Glucose	Glycolysis/Gluconeogenesis
G-6P	Glucose-6-phosphate	Glycolysis/Gluconeogenesis
F-1,6-BP	Fructose-1,6-biphosphate	Glycolysis/Gluconeogenesis
GAP/ DHAP	Glyceraldehyde 3-phosphate/ dihydroxyacetone phosphate	Glycolysis/Gluconeogenesis
PEP	Phosphoenolpyruvate	Glycolysis/Gluconeogenesis
Pyruvate	Pyruvate	Glycolysis/Gluconeogenesis
Lactate	Lactate	Glycolysis/Gluconeogenesis
E4P	Erythrose-4-phosphate	Pentose phosphate pathway (PPP)
Ribu-5P	Ribulose 5-phosphate	Pentose phosphate pathway (PPP)
Ac-CoA	Acetyl-CoA	TCA cycle
Citrate	Citrate	TCA cycle
Isocitrate	Isocitrate	TCA cycle
2-OG	α-ketoglutarate	TCA cycle
Succ-CoA	Succinyl-CoA	TCA cycle
Succ	Succinate	TCA cycle
Fumarate	Fumarate	TCA cycle
Malate	Malate	TCA cycle
OAA	Oxaloacetate	TCA cycle
Mal-CoA	Malonyl-CoA	Lipogenesis
NAD+	NAD+	Energy metabolism
NADH	NADH	Energy metabolism
NADP+	NADP+	Energy metabolism
NADPH	NADPH	Energy metabolism
ATP	ATP	Energy metabolism
ADP	ADP	Energy metabolism
AMP	AMP	Energy metabolism
Gly	Glycine	Amino acid
Ala	Alanine	Amino acid
Ser	Serine	Amino acid
Pro	Proline	Amino acid
Val	Valine	Amino acid
Thr	Threonine	Amino acid
Leu	Leucine	Amino acid
Ile	Isoleucine	Amino acid
Asn	Asparagine	Amino acid
Asp	Aspartate	Amino acid
Gln	Glutamine	Amino acid
Glu	Glutamate	Amino acid
Met	Methionine	Amino acid
His	Histidine	Amino acid
Phe	Phenylalanine	Amino acid
Arg	Arginine	Amino acid
Tyr	Tyrosine	Amino acid
Trp	Tryptophan	Amino acid
Lys	Lysine	Amino acid

Short name	Full metabolite name	Pathway/Class
C0	Carnitine	Carnitines
C2	Acetyl-L-carnitine	Carnitines
C3	Propionyl-L-carnitine	Carnitines
C4	Butyryl-L-carnitine	Carnitines
C5	Valeryl-L-carnitine	Carnitines
C6	Hexanoyl-L-carnitine	Carnitines
C8	Octanoyl-L-carnitine	Carnitines
C9	Nonayl-L-carnitine	Carnitines
C10	Decanoyl-L-carnitine	Carnitines
C12	Dodecanoyl-L-carnitine	Carnitines
C14	Tetradecanoyl-L-carnitine	Carnitines
C16	Hexadecanoyl-L-carnitine	Carnitines
C16:1	Hexadecenoyl-L-carnitine	Carnitines
C18	Octadecanoyl-L-carnitine	Carnitines
C18:1	Octadecenoyl-L-carnitine	Carnitines